

TEVATRON MAGNETS AND ORBIT VIBRATIONS

V. Shiltsev, T. Johnson, X.L. Zhang, FNAL, Batavia, IL 60510, USA

Abstract

We report results of recent measurements of vibrations of the Tevatron collider elements and orbit movements over large diapason of frequencies.

1 INTRODUCTION

Motion of the beam orbit in the Tevatron can lead to a significant deterioration of the collider performance and, thus, is subject of interest. Motion of quadrupole magnets is one of the major causes of the orbit movements. As the result of orbit drifts from empirically found “good” orbits, significant changes in the betatron frequencies may occur that lead to (usually) higher losses of antiprotons and protons. At the injection energy of 150 GeV when the beams are several mm wide, orbit motion of about a mm leads to losses of the beams at several known places with tight aperture. At the energy of experiment, 980 GeV/beam, beam position in the RF cavities affects stability of high-intensity proton beam, e.g. the power of coherent beam oscillations goes up if the beam is too far off center. Also, oscillations of the RF cavities at synchrotron frequency (85 Hz at 150 GeV and 35 Hz at 980 GeV) are of concern for driving longitudinal emittance growth due to microphonic effects, though direct evidences of the effect are not yet found.

Previous measurements at Fermilab [1,2] were focused on high-frequency vibrations from few Hz to hundred(s) of Hz. Here we present some results of longer term measurements as well as recent data on high-frequency vibrations measured during Run II (March 2001 to present).

2. SLOW ORBIT DRIFTS

Fig.1 shows variations of the Tevatron proton vertical and horizontal orbits during a typical store #1668 started at 2pm August 17, 2002. The orbit is measured by the BPMs of the Tevatron Electron Lens [3] located at sector F48 where beta function is about 100 m horizontal and 30 m vertical. The BPMs report every minute with a resolution of about 10 μm rms. RMS of the orbit motion is 93 μm horizontally and 33 μm vertically. The orbit motion has significant (some 0.1 mm vertical and 0.3 mm horizontal) variation with a period of 12 hrs, which might be associated with Earth tides. The tide waves are clearly seen in the data from the Hydrostatic Level System (HLS) installed in the MI-8 beam line, the 8 GeV transfer line from the FNAL Booster to the FNAL Main Injector, located within 400 m of the Tevatron tunnel. (See the FNAL site map in Fig.2.) The HLS is described in detail in [4] and consists of 20 water level sensors separated by 15 m from one another. The signal difference for a pair of

sensors 135 m apart is shown in the bottom plot of Fig.1. 12 hour oscillations due to tides are within $\pm 10 \mu\text{m}$. Earth tide strain led to LEP circumference and beam energy variation as reported in Ref.[5].

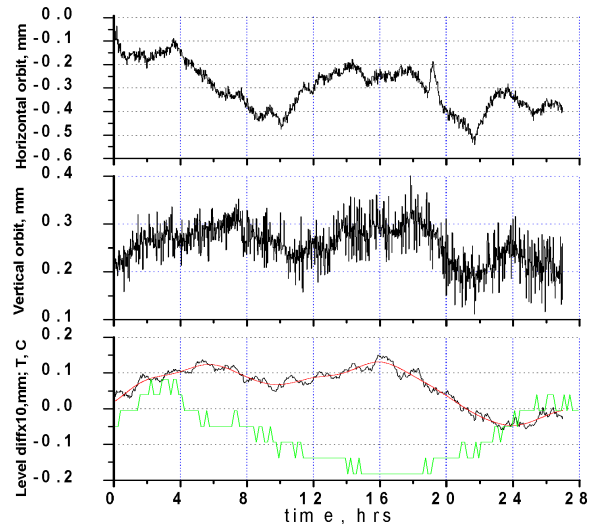


Figure 1: Variation of the Tevatron proton orbits (horizontal – top, vertical – middle), vertical ground motion in MI-8 line and temperature measured at sector F48 (both in bottom plot) during collider store #1668.

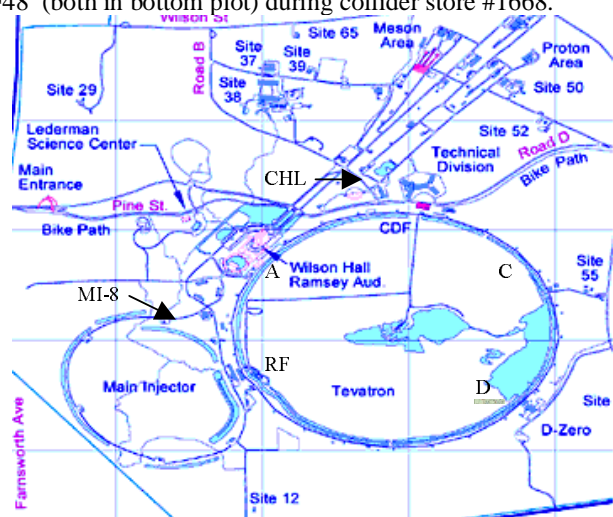


Figure 2: Fermilab site with locations mentioned in the text (to scale – the Tevatron radius is equal to 1000m).

That mechanism is unlikely in the Tevatron because of its 15 times larger momentum compaction factor, so we think the basic mechanism which couples tides and orbit is relative motion of the low-beta quadrupoles. It is known [1] that low-beta quad displacement can be amplified by 10-30 times in the closed orbit distortion

around the ring, so 10 micron quadrupole movement would result in 100-300 micron orbit drift – in a good agreement with our observations.

Orbit motion also seems to be correlated in part with the tunnel temperature (see green line in the bottom plot of Fig.1, it represents T-21.3 °C) which varies by $\pm 0.1^\circ\text{C}$ with period of 24 hrs. On top of the tides and temperature effects there are some “random walk”-like drifts. The orbit PSD scales as the random walk PSD $\propto 1/f^2$ as shown in Fig.3.

There is a handy “ATL law” [6] which says that the variance (mean square) of random ground motion grows linearly with time interval and distance between observation points. For the point-to-point displacement Δy one has:

$$\langle \Delta y^2 \rangle = A \times T \times L \quad (1)$$

where brackets $\langle \dots \rangle$ stay for average over all possible pairs of data points separated by time interval T and distance L , A is a coefficient. It was found that the diffusion coefficient is not much different for vertical and horizontal movements [7]. For an accelerator with circumference C , such a “random walk”-like drift of quadrupole positions lead to distortion of closed orbits (in both planes) with an rms value around the ring of

$$\langle \Delta Y^2 \rangle = G \times (A \times T \times C) \quad (2)$$

where the coefficient $G \approx 2-5$ depends on the focusing lattice and is calculated for regular FODO lattice in Ref.[8], for the Tevatron lattice parameters excluding IRs $G=3.1$ for average $\beta=50\text{m}$.

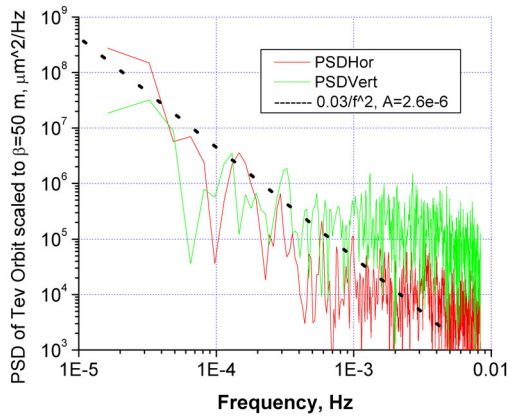


Figure 3: PSD of the orbit motion shown in Fig.1 scaled to beta function of 50 m. Dashed line represents the ATL law prediction $\propto 1/f^2$ (see text).

Corresponding PSD of the rms orbit drifts $Y_{_o}$ is equal to

$$\text{PSD}_{Y_{_o}} = (6GAC) / (\pi^2 f^2) \quad (3)$$

and dashed line in Fig.3 represents such a PSD with the coefficient $A=2.6 \times 10^{-6} \mu\text{m}^2/\text{s/m}$. Such a diffusion coefficient is consistent with the value $A=(1.2 \pm 0.8) \times 10^{-6} \mu\text{m}^2/\text{s/m}$ measured in another Fermilab tunnel of PW beamline [9], and with $A=(1.5 \pm 0.2) \times 10^{-6} \mu\text{m}^2/\text{s/m}$ measured recently in the MI-8 tunnel [4].

Rms orbit drift around the Tevatron due to the ground diffusion with coefficient $A=2 \times 10^{-6} \mu\text{m}^2/\text{s/m}$ is about $0.06 \text{ mm/day}^{1/2}$, or, assuming that peak-to-peak orbit variation is some 3 times the rms value, one gets peak orbit excursion predictions of $0.2 \text{ mm/day}^{1/2}$, $0.5 \text{ mm/week}^{1/2}$, $1 \text{ mm/month}^{1/2}$ and $(3-4) \text{ mm/year}^{1/2}$. These values are not too far from the Tevatron operational experience. Note, that similar type of orbit drifts with $A=(4 \pm 2) \times 10^{-6} \mu\text{m}^2/\text{s/m}$ were observed at HERA [10].

3 EARTHQUAKE

A remarkable event occurred in the Tevatron on June 18, 2002. Around 12:40pm, someone in the offices of the West Booster towers called the MCR to ask if we had felt the building moving. A datalogger plot of the peak-detecting geophone on Tev RF cavity 1 showed a small but definite spike at about the correct time (see pink curve in Fig.4), similar peak occurred in the CDF detector losses (red curve). Checking the USGS web site showed a magnitude 5 quake in Indiana had occurred some two minutes earlier, which was consistent with the surface wave velocity for this region listed on the same site. The location of the epicenter was 9 Km west-southwest of Darmstadt, Indiana (38 deg 4.2 min N, 87 deg 40.8 min W) at a depth of 5.0Km. Time was 1737:13 UTC. Magnitude was 5.0.

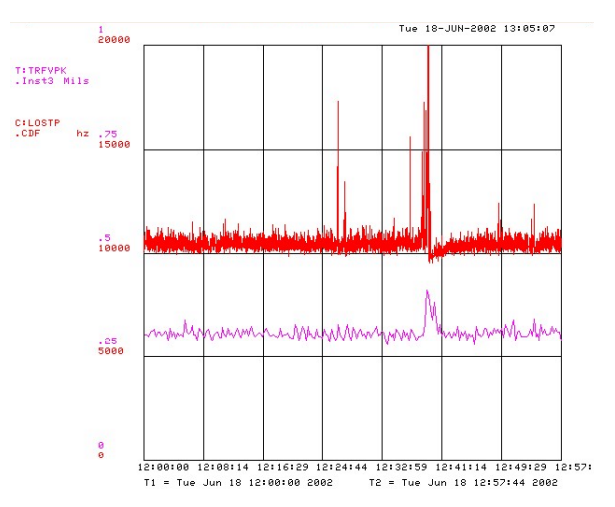


Figure 4: Earthquake signal in the proton losses (red) and in one of accelerometers (pink).

At Fermilab, the amplitude of the waves can be estimated to be about several dozen to 100 μm with period of several seconds. Nevertheless, the measured displacement on the geophone was extremely small, presumably because the motion was well below the lower frequency response of the instrument.

4 HIGH-FREQUENCY VIBRATIONS OF THE MAGNETS AND TEVATRON ORBIT

There several accelerometers used for routine monitoring of vibrations in the Tevatron tunnel. The outer quads of each of the low beta triplets at the D0 interaction region

are fitted with orthogonal pairs of geophones to measure transverse motion. The geophones are GeoSpace model GS-11D, with a frequency response of 4.5 – 1000 Hz and a sensitivity of 0.8V/sec/in. These geophone signals are processed by an integrator module upstairs to produce displacement readings in mils (1mil=0.001inch=25 micron). This module also provides a peak averaged output to allow long term low frequency sampling of the qualitative vibration amplitudes.

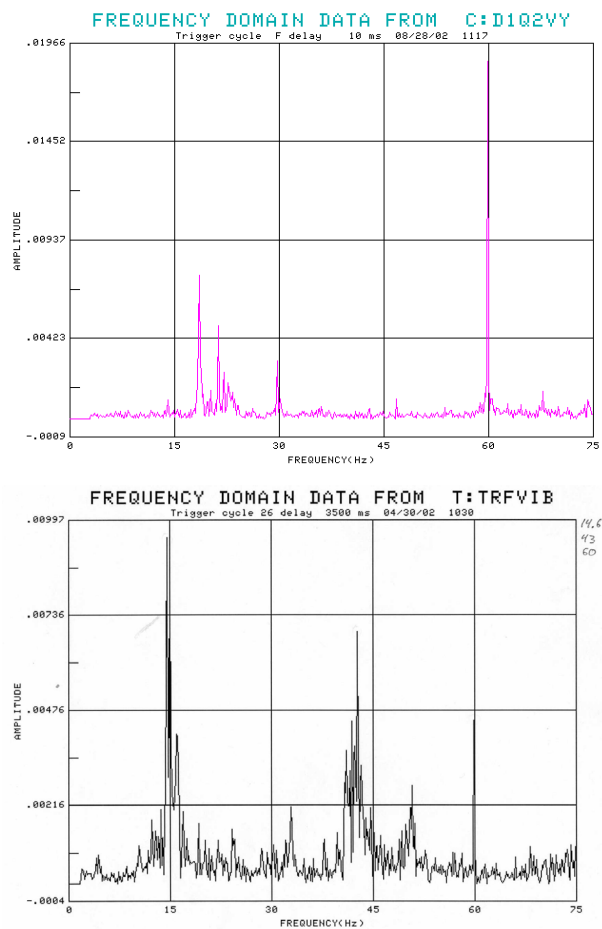
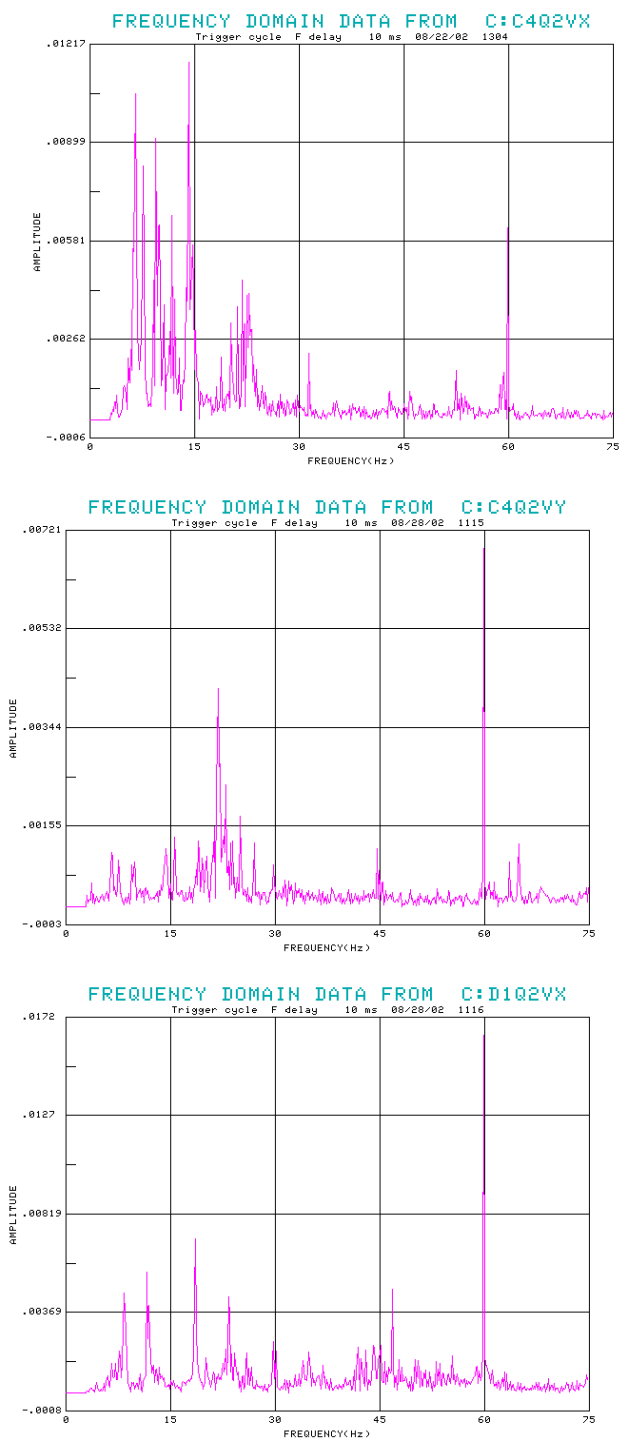


Figure 5: Spectra of mechanical vibrations: top to bottom – horizontal (a), vertical (b) on low-beta quadrupole C4Q2; horizontal (c), vertical (d) on low-beta quadrupole D1Q2, and longitudinal (e) on one of the RF cavities.

The devices are designated by which side of the IR they are (C4 or D1), which quad (Q2) and the axis (Vibration X and Vibration Y). So C:D1Q2VX measures the horizontal displacement of the Q2 magnet on the D1 side. Typical frequency spectra of the mechanical vibrations are presented in Fig.5. These plots may not be completely representative of the vibration the quads experience since measurements made with a real time analyzer show that these frequency peaks “breathe” and exchange energy over a period of a few seconds. The signatures do not vary appreciably with changes in the state of the accelerator, so the motion is believed to be primarily due to ventilation fans. The geophones contain noise canceling windings, however the fringe field gradients at the surface of the quads when ramping is great enough to induce signals of comparable amplitude to the real vibration. Magnetic shielding and high pass filters on the integrator inputs are being investigated to improve the noise immunity of the system.

Vibrations on the C4 side of the IP are usually larger, in part because it is closer to the CHL plant – a known source of ground vibrations on the FNAL site [1,2]. E.g.,

maximum amplitude of C4Q2 vibrations is 0.5 micron horizontally at 6.5Hz and 7.5Hz lines and 0.16 micron vertically at 21.5 Hz line, while maximum amplitude of D1Q2 is 0.16 micron horizontally and vertically at 18.5 Hz. Spectrum of vertical vibrations of the RF cavities – see Fig.5(e) – contains several strong lines at 14.5 Hz (0.25 μm), 15 Hz (0.17 μm), 16 Hz (0.11 μm), 42.6 Hz (0.17 μm) and only 0.02 μm at the CHL line of 4.6 Hz. In general we found that the CHL frequency lines at 4.6, 8.5, 9.2, 13.9 Hz [1,2] are not very prominent at D0 and F0, and typically higher frequency stand/support resonance lines are several times stronger.

The orbit oscillation measurement system is schematically presented in Fig. 6.

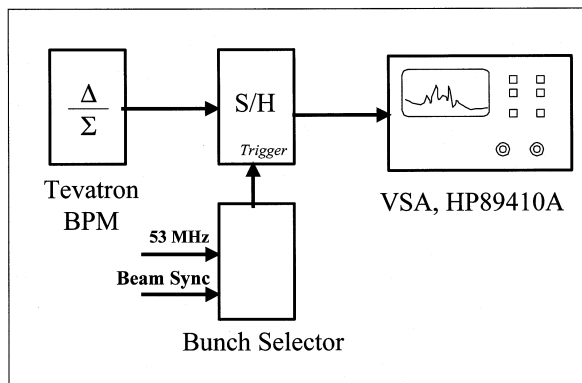


Figure 6: Orbit oscillation measurement system.

We take the beam position signal from the standard Tevatron BPM output at A0, which is calibrated as 12mV/mm. Then this signal is fed into a custom sampling and hold card (S/H card) with a default low pass filter of 10KHz, which is triggered in single bunch mode. The resolution of the delay is 1 RF bucket. The fine adjustment of the delay is done by choosing appropriate cable length for the maximum signal strength with respect to the background noise. Finally, the signal coming out of the S/H card is fed into a vector signal analyzer (VSA) to analyze the beam position signal spectrum. We found that the slow beam orbit spectrum is less than 60Hz so we safely put a 1KHz low pass filter in the S/H card to improve the signal quality. We also saw strong spectrum of the 60Hz and its harmonics coming through the power cord which are not from the beam signal. At A0 BPM location the horizontal and vertical beta-function are about 130m and 85m and dispersions are $D_x=2.315\text{m}$ and $D_y=0.209\text{m}$ respectively. The beam position spectrums obtained at 980GeV High Energy Physics (HEP) store with colliding beams in the range of 0 to 50 Hz are presented in Fig. 7. There are numerous strong lines with 2-10 micron amplitude at 4,6, 6.5, 8.5, 12, 15, 17, 18.5, 23, 34, 35.5 Hz in the horizontal spectrum. The two latter frequencies are due to the synchrotron oscillations of the beam seen at the location with non-zero dispersion when the longitudinal damper was off, which corresponds to a large longitudinal oscillation $\sim 150\text{ps}$ ($\sim 3^\circ$ phase

oscillation). The amplitude difference of the longitudinal signal seen from horizontal and vertical pickups agrees to the dispersion difference of about 24dB. When the longitudinal damper was turned on, these longitudinal signals were completely suppressed.

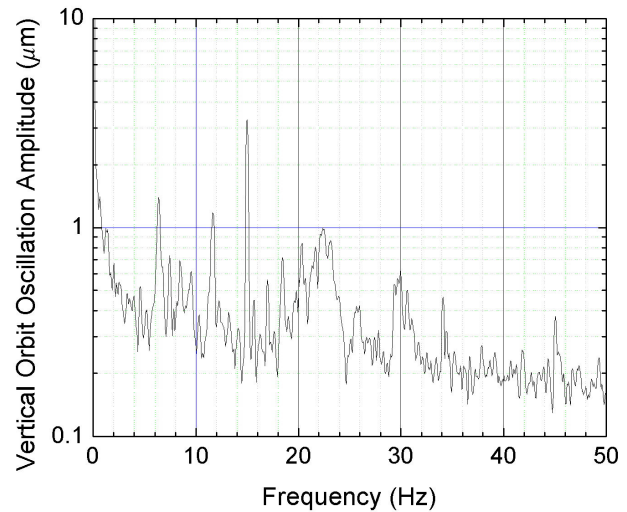
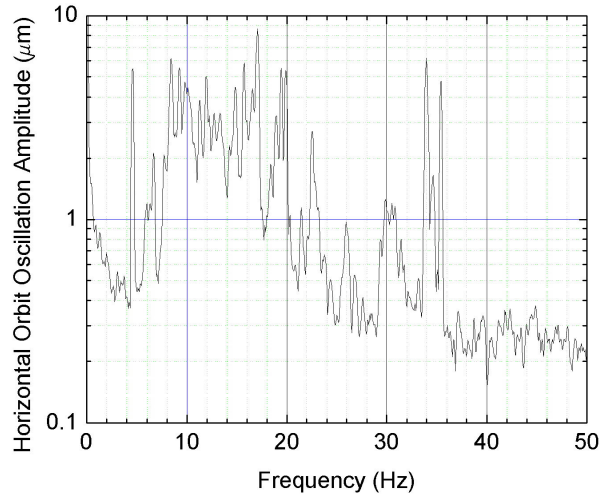


Figure 7: Spectra of horizontal (top) and vertical Tevatron proton beam orbit motion.

The rms horizontal amplitude is about 20 micron. Vertical spectrum is less messy and has >1 micron lines only at 6.5, 11.5, 15, and 23 Hz. The vertical rms amplitude is about 4 micron. In general, beam orbit spectra contain all ground motion lines excited by the CHL, lines associated with mechanical resonances of the supports and synchrotron frequency.

4 CONCLUSION

For the sake of completeness, we present here two plots summarizing previous studies: Fig. 8 shows spectra of the tunnel floor and quadrupole vibrations measured at the A3 sector and reported in Ref.[1], existence of strong correlation between quadrupole vibrations and orbit motion has been experimentally proven in Ref.[2] – see Fig. 9 taken from there.

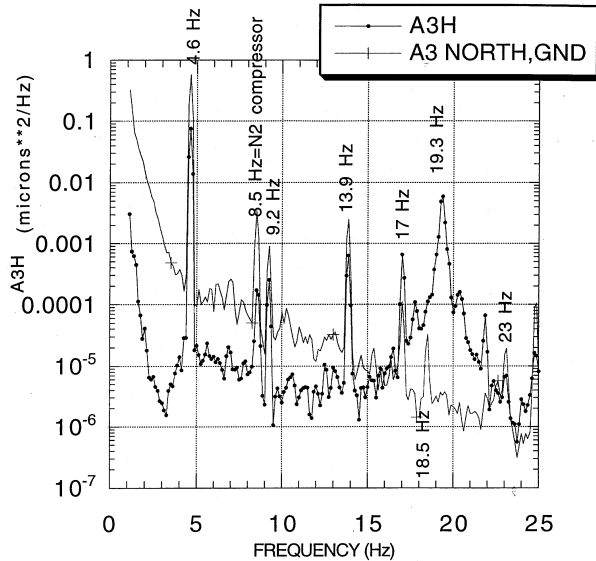


Figure 8: PSD of ground and quadrupole vibrations measured at A3, from [1].

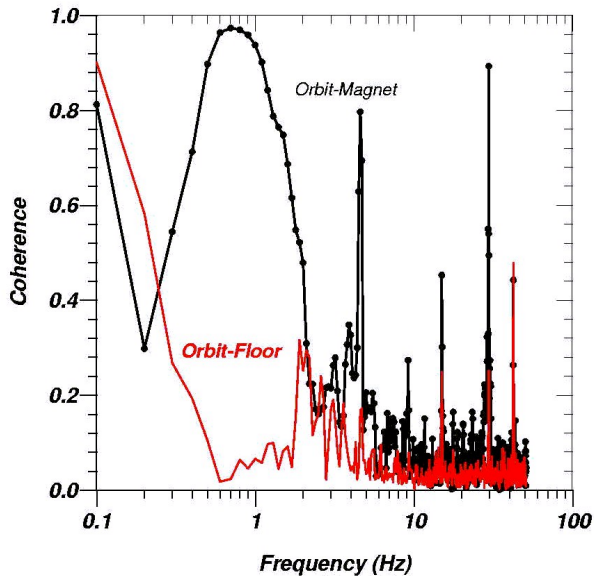


Figure 9: Correlation between proton orbit motion and tunnel floor and magnet vibrations, from [2].

Compared to these previous works, in this article we have considered low-frequency orbit drifts in the Tevatron which contain 24 hour variations due to the temperature changes, 12-hour oscillations correlated with Earth tides and additional random like motion which can be described by the ATL law with coefficient $A=2.6 \times 10^{-6} \mu\text{m}^2/\text{s/m}$. We also observe that only “local” earthquakes may affect the Tevatron operation but they do not occur frequently. Measured spectra of the low-beta quadrupoles and RF cavities vibrations and spectrum of the orbit oscillations contain several frequencies lines previously associated with the CHL operation but in addition many other frequencies. Amplitude of the low-beta quadrupole vibrations at frequencies below 50 Hz does not exceed 0.5 micron while the orbit motion at the same frequencies is some 10-20 microns.

We are thankful to J.Marriner, D.Wildman, C.Y.Tan and J.Steinel for valuable assistance in our studies.

5 REFERENCES

- [1] C.Moore, IWAA95, KEK-Proc-95/12 (1996), p.119
- [2] B.Baklakov, et.al, *Phys.Rev.ST-AB*,1,031001(1998)
- [3] X.L.Zhang, et.al, Proc.BIW'02, BNL (2002).
- [4] V.Shiltsev, et.al, Proc. “Nanobeam-2002” (2002).
- [5] L.Arnaudon, et.al, NIM A 357 (1995), p. 249.
- [6] B.Baklakov, et. al, *Sov.Tech.Phys*, 38 (1998), 894.
- [7] V.Shiltsev, IWAA95,KEK-Proc-95/12(1996), p.352
- [8] V.Parkhomchuk, V.Shiltsev, G.Stupakov, *Particle Accelerators*, v.46 (1994), p.241.
- [9] V.Shiltsev, Proc. IEEE PAC'01 (2001), p.1470.
- [10] R.Brinkmann, J.Rosbach, .NIM, A350 (1994), p.8.